BL12B2
NSRRC BM

BL12B2 is one of the two contract beamlines operated by National Synchrotron Radiation Research Center (NSRRC, Taiwan) under the collaborative research with Japan Synchrotron Radiation Research Institute (JASRI) and RIKEN. Though the beamline was originally designed for materials science and protein crystallography, due to completion of the 3-GeV Taiwan Photon Source (TPS) at NSRRC, the beamtime distribution between these research fields has changed. Currently, > 90% of the beamtime is assigned to material science users, and about 75% of the users are from Taiwan. The rest of the beamtime is shared between international users from Japan and around the world.

Figure 1 schematically depicts the beamline layout. The beamline is equipped with a collimating mirror (CM), a double crystal monochromator (DCM), and a focusing mirror (FM). The measured spot size and total flux of the beam are about 250μm square and about 1.5×10^{11} photons at the protein end-station at an incident photon energy of 12 keV, respectively. Five end-stations, EXAFS, projection X-ray microscopy (PXM), X-ray diffraction, X-ray scattering, and powder X-ray diffraction (powder XRD), are equipped tandemly inside the experimental hutch of BL12B2.

EXAFS experiments are performed at the EXAFS table. The EXAFS spectrum can be measured using both transmission and reflection modes. Temperature-dependent powder X-ray diffraction is measured using an image plate at the XRD table. X-ray scattering experiments can be performed using the HUBER six-circle diffractometer. The sample temperature of these two experiments can be changed from 20 K to 400 K. In 2018, the PXM end station was installed at the XRD table. High-pressure X-ray diffraction is performed using a CCD camera at the protein crystallography table.

The powder X-ray diffraction (powder XRD) end-station, which is equipped with a CCD and SPring-8 standard auto sample-changer system,

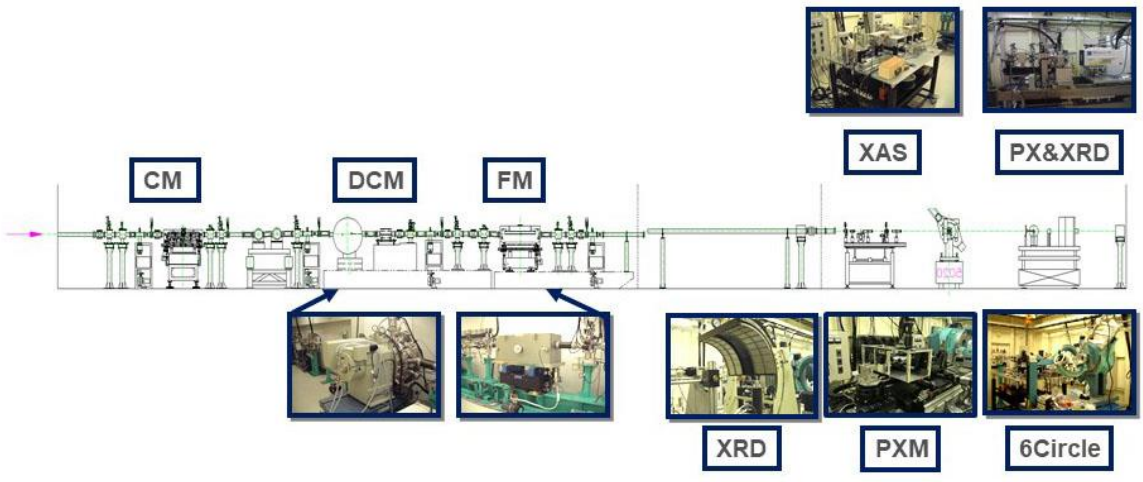

Fig. 1. Schematic layout of BL12B2

was installed in FY2009, and was used for protein diffraction experiments until FY2017. However, beamtime for protein-crystallography users has diminished since FY2017. Currently, the powder XRD end-station is mainly used by material scientists. The user interface software for powder XRD experiments is the SPring-8 standard BSS software. The CCD detector was upgraded to Raynox MX225-HE in FY2014. Electrode (AUTOLAB PGSTAT204 (Metrohm)) was prepared for *in situ* electrochemical experiments.

Materials science experiments cover a wide area of topics such as new material research, energy science, nanoscience, and geophysical science. In FY2019, BL12B2 users published 27 papers in SCI journals.

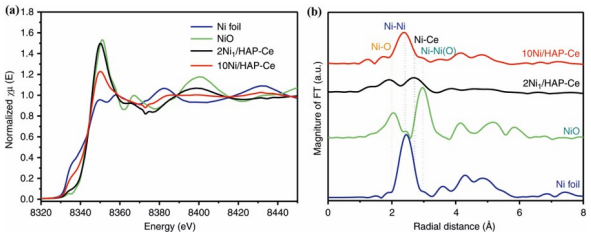

Fig. 2. X-ray adsorption spectroscopy study of Ni/HAP-Ce catalysts. (a) Ni K-edge XANES spectra of 500 °C reduced HAP-Ce–supported Ni catalysts and reference samples, and (b) the corresponding phase shift corrected k2-weighted Fourier transform [21].

BL12B2 is often used for *in situ* X-ray experiments for research on electrocatalysis such as battery research, oxygen reduction reaction, and CO_2 conversion. Recently, the electrochemical conversion of CO_2 to chemical fuel has become an important and promising strategy for global carbon balance. Prof. H-M. Chen (Taiwan Univ.) and colleagues have studied this topic widely [3-7,9,10,12,13,16,17,20,27]. Additionally, Prof. T. Zhang (Chinese Academy of Sciences) measured the Ni K-edge EXAFS and published, "Atomically dispersed nickel as coke-resistant active sites for methane dry reforming" on Nature Communications [21].

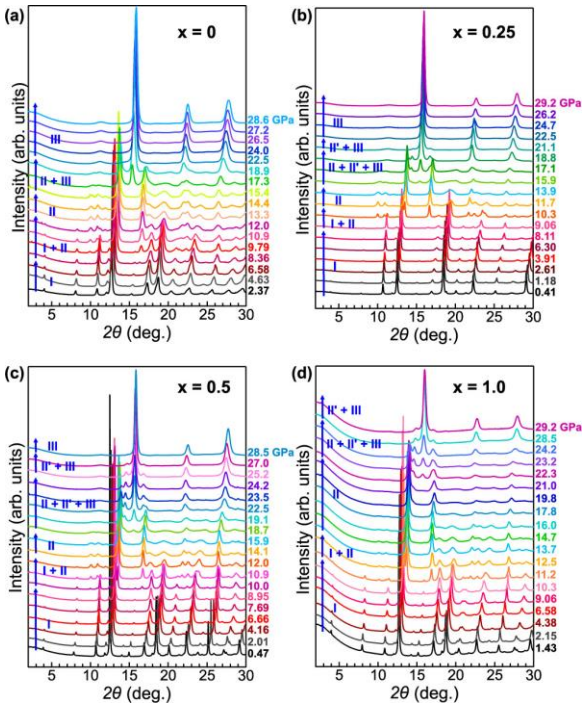

Fig. 3. Pressure-dependent powder XRD patterns of $Bi_{2-x}Sb_xTe_2Se$ with nominal x values

Other studies have focused on samples under extreme conditions to investigate new physical phenomenon. Research on a new type of superconductivity is a hot topic in the field of solid-state physics. Figure 3 shows the pressure-dependent XRD spectrum of a topological insulator $Bi_{2-x}Sb_xTe_2Se$ upon substituting bismuth with antimony, which exhibits superconductivity at 2.0 K [24]. This same group also studied XRD on other samples exhibiting superconducting properties [19,22,23].

User support is provided by three local beamline scientists and one engineer.

Y.-F. Liao, M. Yoshimura, T. Tatsumi and H. Ishii
NSRRC, Taiwan

References:

[1] Gandhi,A. C. et al. (2019). Concomitant Magnetic Memory Effect in CrO2-Cr2O3 Core-shell Nanorods: Implications for Thermal Memory Devices. *ACS Appl. Nano Mater*., 2, 8027.

[2] Deng, M.-J. et al. (2019). 3D Network V2O5 Electrodes in a Gel Electrolyte for High-voltage Wearable Symmetric Pseudocapacitors. ACS Appl. Mater. Interfaces, 11, 29838.

[3] Wang, S.-Y. et al. (2019). Defect Passivation by Amide-based Hole-transporting Interfacial Layer Enhanced Perovskite Grain Growth for Efficient p-i-n Perovskite Solar Cells. ACS Appl. Mater. Interfaces, 11, 40050.

[4] Suen, N.-T. et al. (2019). Morphology Manipulation of Copper Nanocrystals and Product Selectivity in the Electrocatalytic Reduction of Carbon Dioxide. ACS Catalysis, 9, 5217.

[5] Chang, C.-J. et al. (2019). Quantitatively Unraveling the Redox Shuttle of Spontaneous Oxidation/Electroreduction of CuOx on Silver Nanowires Using in Situ X-ray Absorption Spectroscopy. ACS Central Sci., 5, 1998.

[6] Song, F. et al. (2019). An Unconventional Iron Nickel Catalyst for the Oxygen Evolution Reaction. ACS Central Sci., 5, 558.

[7] Hung, S.-F. et al. (2019). In Situ Spatially Coherent Identification of Phosphide-based Catalysts: Crystallographic Latching for Highly Efficient Overall Water Electrolysis. ACS Energ. Lett., 4, 2813.

[8] Sarkar, C. et al. (2019). Integration of Interfacial and Alloy Effects to Modulate Catalytic Performance of Metal-organic-framework-derived Cu-Pd Nanocrystals Toward Hydrogenolysis of 5-Hydroxymethylfurfural. ACS Sustain. Chem. Eng., 7, 10349.

[9] Chu, Y.-C. et al. (2019). Anionic Effects on Metal Pair of Se-doped Nickel Diphosphide for Hydrogen Evolution Reaction. ACS Sustain. Chem. Eng., 7, 14247.

[10] Chen, R. et al. (2019). Layered Structure Causes Bulk NiFe Layered Double Hydroxide Unstable in Alkaline Oxygen Evolution Reaction. Adv. Mater., 31, 1903909.

[11] Chen, L. et al. (2019). Reduced Local Symmetry in Lithium Compound Li2SrSiO4 Distinguished by an Eu3+ Spectroscopy Probe. Adv. Sci., 6, 1802126.

[12] Ni, W. et al. (2019). Ni3N as an Active Hydrogen Oxidation Reaction Catalyst in Alkaline Medium. Angew. Chem. Int. Edit., 58, 7445.

[13] Chang, C.-J. et al. (2019). Revealing the Structural Transformation of Rutile RuO2 via in Situ X-ray Absorption Spectroscopy During the Oxygen Evolution Reaction. Dalton T., 48, 7122.

[14] Hsu, L.-C. et al. (2019). Adsorption Mechanisms of Chromate and Phosphate on Hydrotalcite: A Combination of Macroscopic and Spectroscopic Studies. Environ. Pollut., 247, 180.

[15] Huang, E.-W. et al. (2019). Deviatoric Deformation Kinetics in High Entropy Alloy Under Hydrostatic Compression. J. Alloy. Compd., 792, 116.

[16] Bai, L. et al. (2019). A Cobalt-iron Double-atom Catalyst for the Oxygen Evolution Reaction. J. Am. Chem. Soc., 141, 14190.

[17] Gao, et al. (2019). Breaking Long-range Order in Iridium Oxide by Alkali Ion for Efficient Water Oxidation. J. Am. Chem. Soc., 141, 3014.

[18] Huang, S.-C. et al. (2019). Vanadium-based Polyoxometalate as Electron/Ion Sponge for Lithium-ion Storage. J. Power Sources, 435, 226702.

[19] Yang, X. et al. (2019). Preparation and Characterization of a New Metal-intercalated Graphite Superconductor. Mater. Res. Exp., 6, 016003.

[20] Jiao, J. et al. (2019). Copper Atom-pair Catalyst Anchored on Alloy Nanowires for Selective and Efficient Electrochemical Reduction of CO2. Nat. Chem., 11, 222.

[21] Akri, M. et al. (2019). Atomically Dispersed Nickel as Coke-resistant Active Sites for Methane Dry Reforming. Nat. Commun., 10, 5181.

[22] Horigane, K. et al. (2019). Superconductivity in a New Layered Triangular-lattice System Li2IrSi2. New J. Phys., 21, 093056.

[23] Yang, X. et al. (2019). Superconducting Properties of (NH3)yLixFeSe0.5Te0.5 Under Pressure. New J. Phys. 21, 113010.

[24] He, T. et al. (2019). Pressure-induced Superconductivity in Bi2−xSbxTe3−ySey. Phys. Rev. B, 100, 094525.

[25] Okamoto, H. et al. (2019). Synthesis of the extended phenacene molecules, [10]phenacene and [11]phenacene, and their performance in a field-effect transistor. Sci. Rep., 9, 4009.

[26] Hu, C.-W. et al. (2019). Cyclability Evaluation on Si Based Negative Electrode in Lithium Ion Battery by Graphite Phase Evolution: an Operando X-ray Diffraction Study. Sci. Rep., 9, 1299.

[27] Gu, J. et al. (2019). Atomically Dispersed Fe3+ Sites Catalyze Efficient CO2 Electroreduction to CO. Science, 364, 1091.